

Supporting Information

Instantly High-Selectivity Cd-MOF Chemosensor for Naked-Eye Detection of Cu(II) Approved by *in situ* Microcalorimetry

Chengfang Qiao,^{a,b} Xiaoni Qu,^a Qi Yang,^a Qing Wei,^a Gang Xie,^a Sanping Chen,^{*a} Desuo
Yang^c

[a] Key Laboratory of Synthetic and Natural Functional Molecule Chemistry of Ministry of Education, College of
Chemistry and Materials Science, Northwest University, Xi'an 710127, P. R. China

[b] Shaanxi Key Laboratory of Comprehensive Utilization of Tailings Resources, College of Chemical
Engineering and Modern Materials, Shangluo University, Shangluo 726000, P. R. China

[c] College of Chemistry and Chemical Engineering, Baoji University of Arts and Sciences, Baoji 721013, P. R.
China

Corresponding author

Prof. Sanping Chen

E-mail: sanpingchen@126.com

Table of contents

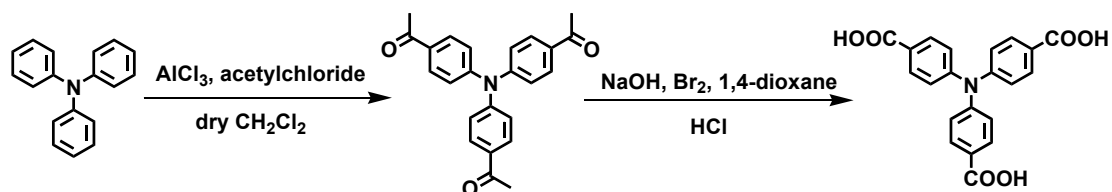
- Fig. S1** ^1H NMR (400 MHz, CDCl_3) spectrum of triacetyltriphenylamine.
- Fig. S2** ^1H NMR (400 MHz, $\text{DMSO-}d_6$) spectrum of tricarboxyltriphenylamine (H_3L).
- Fig. S3** ^{13}C NMR (126 MHz, $\text{DMSO-}d_6$) spectrum of tricarboxyltriphenylamine (H_3L).
- Fig. S4** 3D framework of **1** (a) assembled *via* 2D wave-like double sheet structures (b), which were generated by two kinds of L^{3-} ligands (blue and pink balls) bridging pentanuclear Cd(II) cluster nodes (green balls). All H atoms, counter ions and solvent molecules are omitted for clarity.
- Fig. S5** View of the 3D framework of **1** shown in Ball-Stick mode (a) and Spacefill mode (b) along the *a*-axis. All H atoms, counter ions and solvent molecules are omitted for clarity.
- Fig. S6** View of the 3D framework of **1** shown in Ball-Stick mode (a) and Spacefill mode (b) along the *b*-axis. All H atoms, counter ions and solvent molecules are omitted for clarity.
- Fig. S7** View of the 3D framework of **1** shown in Ball-Stick mode (a) and Spacefill mode (b) along the *c*-axis. All H atoms, counter ions and solvent molecules are omitted for clarity.
- Fig. S8** Powder XRD patterns of (a) **1**, **1'**, **1**·DMA and **1**· CH_3OH ; (b) **2** and its simulated one.
- Fig. S9** The corresponding Gram–Schmidt signal of **1**· CH_3OH and **1**·DMA.
- Fig. S10** Gas phase IR spectra corresponding to the maximum of the Gram–Schmidt signal in Fig. 9 of (a) **1**· CH_3OH and (b) **1**·DMA as well as reference spectra of (c) methanol and (d) N-dimethylacetamide.
- Fig. S11** TG curves for **1**, **1**· CH_3OH and **1**·DMA under a nitrogen atmosphere.
- Fig. S12** (a) Variation of heat-flow as a function of time, **1**· CH_2Cl_2 , **1**· CHCl_3 , **1**· CCl_4 , **1**·benzene, and **1**·cyclohexane, (b) **1**· CH_3OH and **1**·DMA.
- Fig. S13** Changes in color of addition of various metal ions ($1 \times 10^{-4} \text{ mol L}^{-1}$, 10 mL) to the crystals of **1**.
- Fig. S14** (a) Coordination environments of the Cd(II) and Cu(II) ions in **2**. Symmetry code: A, $-x+1, -y, -z+2$; (b) Two different types of coordination modes of L^{3-} ligand in **2**. Symmetry code: A, $x, y, z+1$; B, $-x+1, y-1/2, -z+5/2$; C, $-x+1, y+1/2, -z+3/2$; D, $x+1, y, z$; (c) View of the 3D framework of **2** shown in Ball-Stick mode along the *c*-axis. All H atoms, counter ions and solvent molecules are omitted for clarity.
- Fig. S15** (a) Variation of heat-flow as a function of time, $c(\text{Cu}^{2+})=1 \times 10^{-5} \text{ mol L}^{-1}$, (b) $c(\text{Cu}^{2+})=1 \times 10^{-6} \text{ mol L}^{-1}$.
- Fig. S16** Change in absorption intensity of **1** ($1 \times 10^{-5} \text{ M}$) in DMSO upon addition of various metal ions (10 mM).
- Fig. S17** Emission spectra of **1** in DMSO with $\text{Cu(NO}_3)_2$ at different concentrations.
- Table S1** Crystal data and refinement parameters for compounds **1**, **2**, **1**· CH_3OH and **1**·DMA.

1. Experimental

1.1. Materials and instrumentation

The H₃L ligand was synthesized by the literature method.^[S1] All other reagents were reagent grade and used as purchased without further purification. ¹H NMR spectra were recorded at 400 MHz and ¹³C NMR spectrum was recorded on Varian INOVA 500M spectrometer. Tetramethylsilane (TMS) served as internal reference ($\delta = 0$) for ¹H NMR, and DMSO-*d*₆ served as internal standard ($\delta = 39.51$) for ¹³C NMR. Elemental analyses of C, H, and N were performed on a Vario EL III analyzer fully automated trace element analyzer. The FT-IR spectra were recorded on a Nicolet Magna 750 FT-IR spectrometer using KBr pellets in the range of 4000-400 cm⁻¹. Fluorescent data were collected on an Edinburgh FLS920 TCSPC fluorescence spectrophotometer equipped with 450W xenon light. Inductively coupled plasma (ICP) analysis was performed on a Perkin–Elmer Optima 3300 DV ICP spectrometer. Thermogravimetric analysis was investigated using a thermogravimetric analyzer at first. The gaseous products from the samples during heating under N₂ atmosphere were analyzed by an online FTIR (Bruker, Vertex70) with a 200 ml gas cell in the range of 400-4000cm⁻¹. The phase purity of the bulk sample was verified by X-ray powder diffraction (XRPD) radiation ($\lambda = 1.5406 \text{ \AA}$), with a scan speed of 5° min⁻¹ and a step size of 0.02° in 2 θ . The calorimetric experiment was performed by using a RD496-III type microcalorimeter.^[S2] The calorimetric constants at 295.15, 298.15, 301.15, 304.15, and 307.15 K were determined, by the Joule effect, to be 63.799 ± 0.025, 63.901 ± 0.030, 64.000 ± 0.026, 64.075 ± 0.038, and 64.203 ± 0.043 $\mu\text{V} \cdot \text{mW}^{-1}$, respectively. The enthalpy of the dissolution of KCl (spectral purity) in deionized water was measured to be 17.238 ± 0.048 kJ · mol⁻¹, which is in good agreement with the value of 17.241 ± 0.018 kJ · mol⁻¹ from ref [S3]. The accuracy is 0.02%, and the precision is 0.3%, which indicates that the calorimetric system is accurate and reliable. The reaction solvent (5 mL) was put into a stainless steel sample cell in a 15 mL container.^[S4] At equilibrium, the containers of the single crystal samples (20-22 mg) were pushed down simultaneously. As a result, the crystal solvent was mixed at 298.15 K, and the thermogram of the crystalline-state-liquid guest exchange was recorded.

1.2. Synthesis of tricarboxytriphenylamine (H_3L)^[S1]



Synthesis of triacetyltriphenylamine

To the solution of $AlCl_3$ (1.8 g, 13.5 mmol) in 50 ml dry CH_2Cl_2 , 2.0 ml (28.28 mmol) acetyl chloride in 50 ml dry CH_2Cl_2 was added dropwisely under 0 °C. The reaction mixture was allowed to warm to room temperature and triphenylamine (1.0 g, 4.0 mmol) in 50 ml dry CH_2Cl_2 was added. Then the reaction was carried out at room temperature for 24 h. The mixture was poured into ice-water (200 mL), and extracted with CH_2Cl_2 (3×100 mL), the organic layer was washed with water (5×100 mL), dried with Na_2SO_4 . After filtration and removal of the solvent under reduced pressure, the crude product was purified by column chromatography with CH_2Cl_2 as an eluent to give a yellow solid (1.20 g, 80.8%). 1H NMR (400 MHz, $CDCl_3$), δ (ppm): 7.91 (d, $J=8.8$, 6H), 7.16 (d, $J=8.7$, 6H), 2.59 (s, 9H).

Synthesis of tricarboxyltriphenylamine

3 mL Br_2 were added dropwisely to the solution of $NaOH$ (7 g, 0.18 mol) in 30 ml water on ice bath. The mixture was stirred for 20 min and added dropwisely to a solution of triacetyltriphenylamine (2.0 g, 5.4 mmol) in 50 ml 1, 4-dioxane. Then the reaction mixture was allowed to warm to room temperature over 1 h and further stirred at 50 °C for 12 h. After cooling to r.t., the mixture was put on ice-bath, saturated hydroxylamine hydrochloride was added to deoxidize excessive sub-bromo-sodium. The solution was acidified by HCl (2M) and the solid product was filtered and dried under vacuum. The crude was recrystallized from acetic acid to afford pure products as a white solid. (1.56 g, 76.5%). Anal. calcd. for $C_{24}H_{21}NO_3$: C, 77.61; H, 5.70; N, 3.77. Found: C, 77.68; H, 5.76; N, 3.71. 1H NMR (400 MHz, $DMSO-d_6$), δ (ppm): 12.85 (s, 3H), 7.92 (d, $J=8.7$, 6H), 7.15 (d, $J=8.7$, 6H). ^{13}C NMR (126 MHz, $DMSO-d_6$) δ (ppm): 166.81, 149.88, 131.25, 125.93, 123.78.

1.3. Synthesis of $\{[NH_2(CH_3)_2][Cd_{2.5}(L)_2(H_2O)] \cdot (H_2O)\}_n$ (1).

A mixture of H₃L (37 mg, 0.1 mmol), CdSO₄·8/3H₂O (51 mg, 0.2 mmol), N,N-dimethylformamide (5 mL), acetone (4 mL) and water (3 mL) were placed in a 25 mL Teflon liner. The resulting mixture was stirred for 30 min at room temperature, and then the mixture was sealed in a Parr autolave and kept at 100°C for 3 days and then cooled to room temperature at a rate of 5 °C min⁻¹. Yellow block crystals of **1** were obtained in 47% yield (based on H₃L). Anal. Calcd for C₈₈H₇₂Cd₅N₆O₂₈ (2223.52): C, 47.36; H, 3.25; N, 3.77%. Found: C, 47.06; H, 3.49; N, 3.92%. IR (cm⁻¹): 3446 (s), 1590 (s), 1527 (m), 1391 (s), 1318 (m), 1264 (m), 1173 (w), 1104(w), 862 (w), 791 (m), 710 (w), 682 (w).

1.4. X-ray structure determinations

Diffraction intensities of all compounds were collected on a Rigaku SCX mini CCD diffractometer using graphite-mono-chromatized MoK α radiation ($\lambda = 0.71073 \text{ \AA}$) at room temperature. The data integration and reduction were processed with SAINT software. Absorption correction based on multi-scan was performed using the SADABS program.^[S5] The structures were solved by the direct method using SHELXTL and refined by a full-matrix least-squares method on F^2 with the SHELXL-97 program.^[S6] All non-hydrogen atoms were refined anisotropically. A summary of the crystallographic data and data collection, refinement parameters are listed in Table S1.

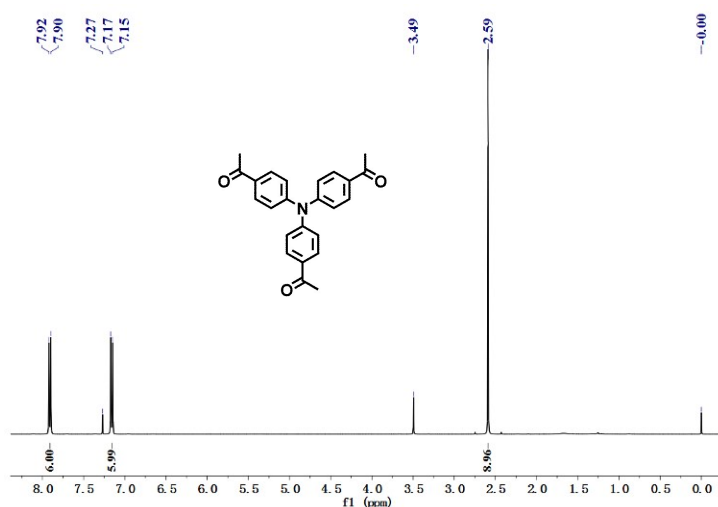


Fig. S1 ¹H NMR (400 MHz, CDCl₃) spectrum of triacetyltriphenylamine.

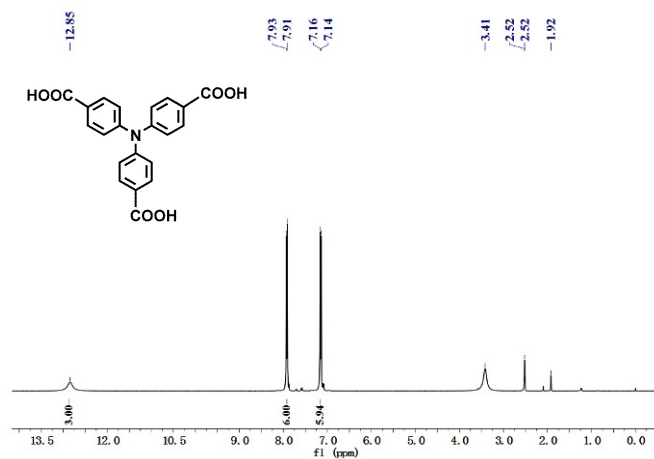


Fig. S2 ^1H NMR (400 MHz, $\text{DMSO-}d_6$) spectrum of tricarboxyltriphenylamine (H_3L).

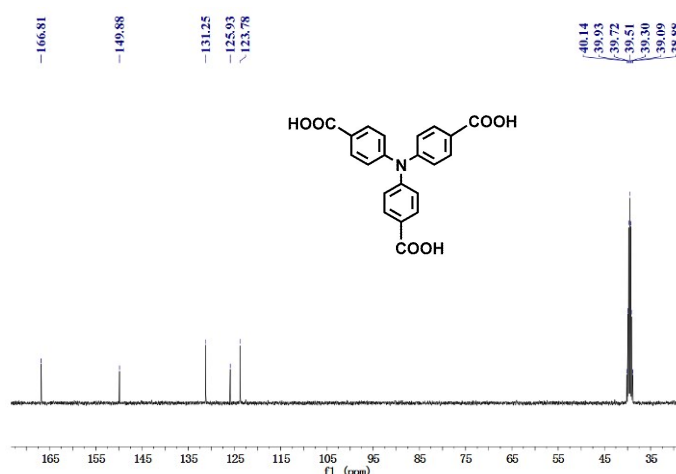


Fig. S3 ^{13}C NMR (126 MHz, $\text{DMSO-}d_6$) spectrum of tricarboxyltriphenylamine (H_3L).

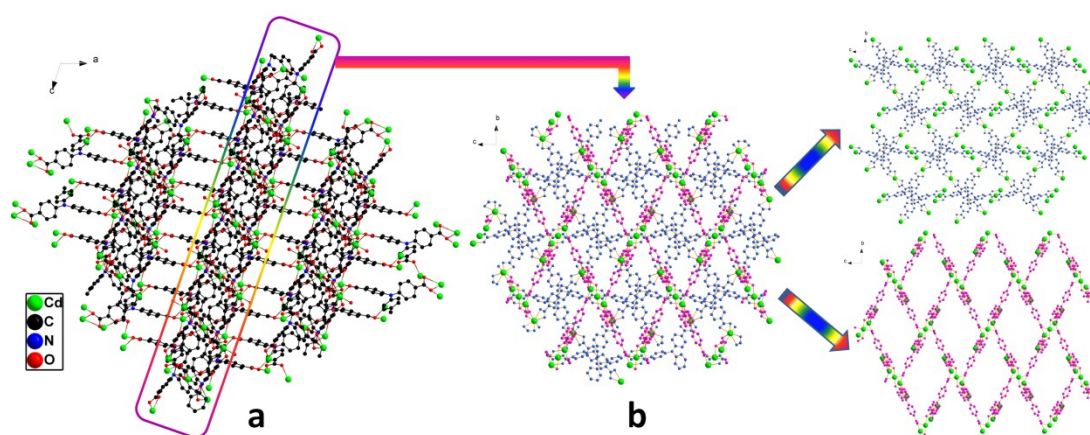


Fig. S4 3D framework of **1** (a) assembled *via* 2D wave-like double sheet structures (b), which were generated by two kinds of L^3 -ligands (blue and pink balls) bridging pentanuclear $\text{Cd}(\text{II})$ cluster nodes (green balls). All H atoms, counter ions and solvent molecules are omitted for clarity.

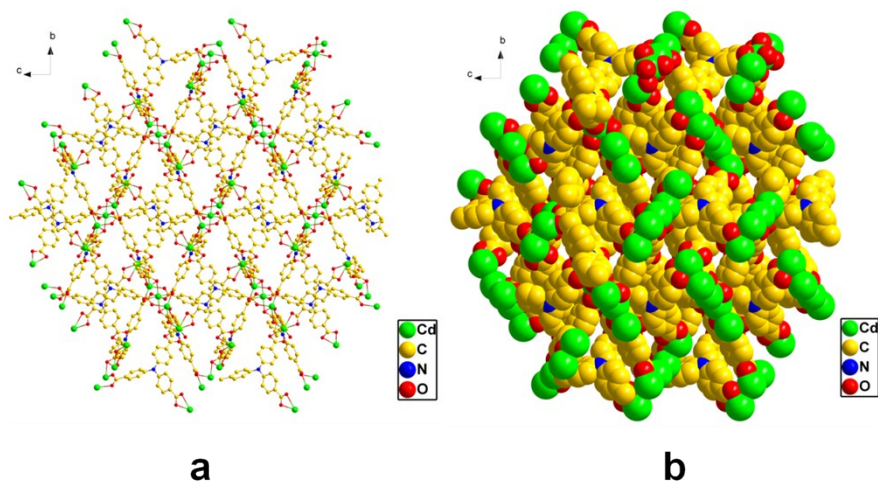


Fig. S5 View of the 3D framework of **1** shown in Ball-Stick mode (a) and Spacefill mode (b) along the *a*-axis. All H atoms, counter ions and solvent molecules are omitted for clarity.

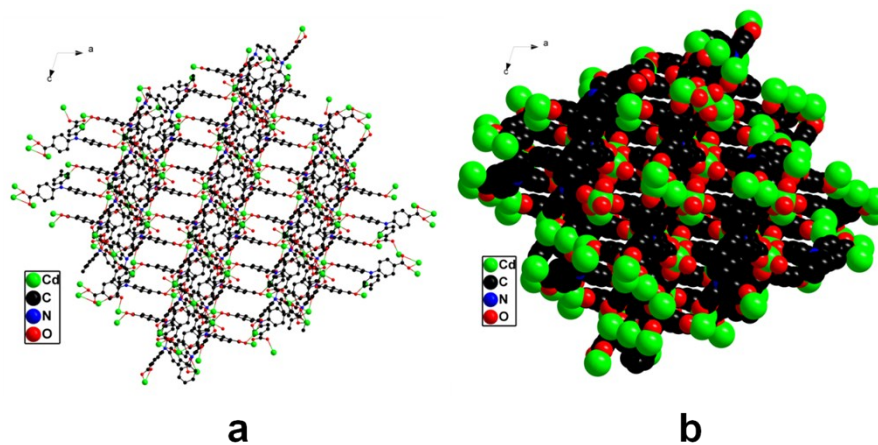


Fig. S6 View of the 3D framework of **1** shown in Ball-Stick mode (a) and Spacefill mode (b) along the *b*-axis. All H atoms, counter ions and solvent molecules are omitted for clarity.

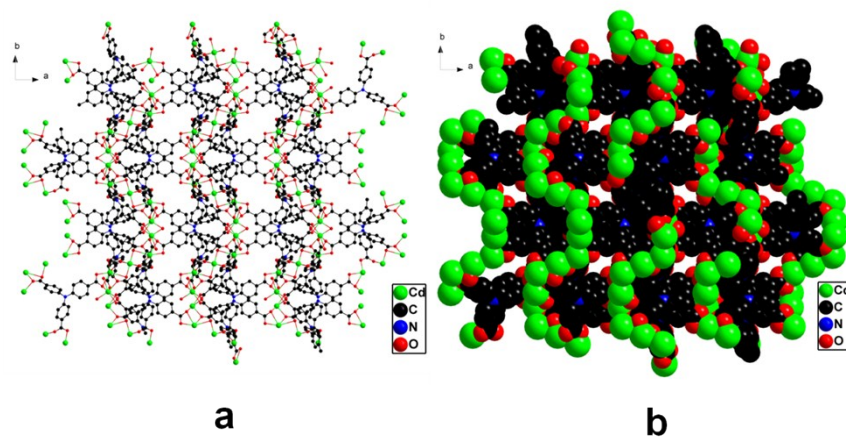


Fig. S7 View of the 3D framework of **1** shown in Ball-Stick mode (a) and Spacefill mode (b) along the *c*-axis. All H atoms, counter ions and solvent molecules are omitted for clarity.

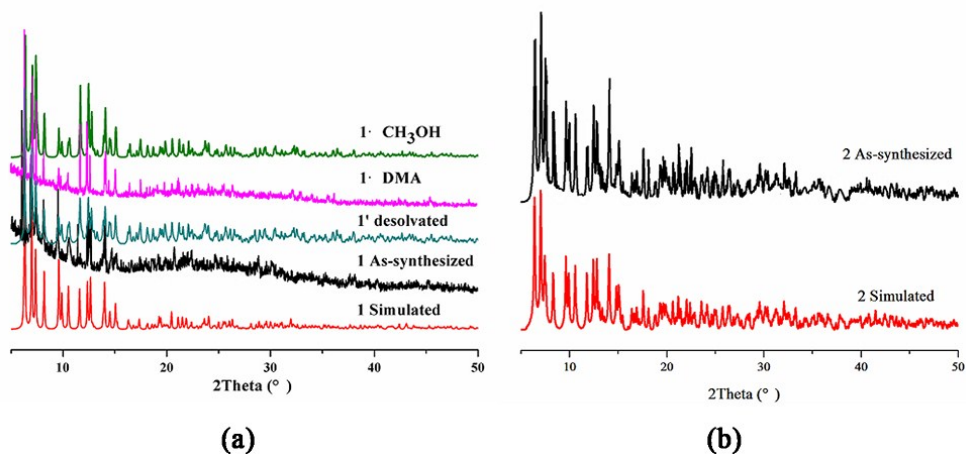


Fig. S8 Powder XRD patterns of (a) **1**, **1'**, **1·DMA** and **1·CH₃OH**; (b) **2** and its simulated one.

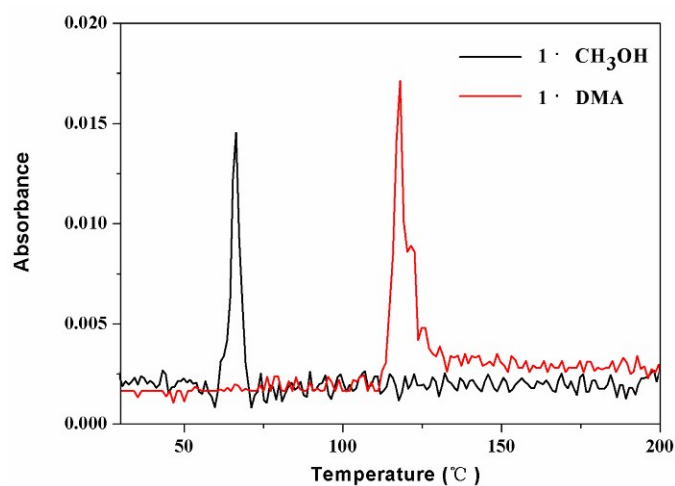


Fig. S9 The corresponding Gram-Schmidt signal of **1·CH₃OH** and **1·DMA**.

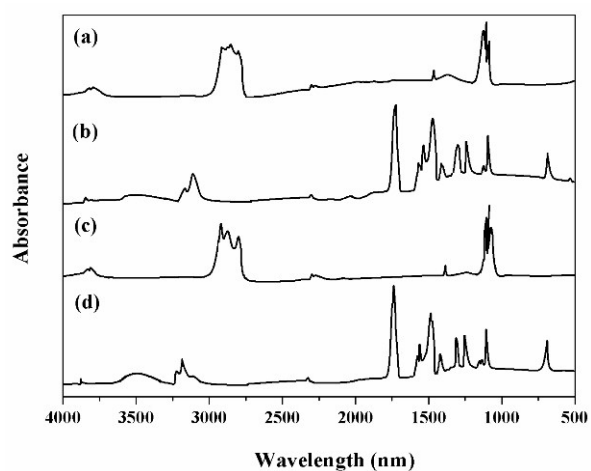


Fig. S10 Gas phase IR spectra corresponding to the maximum of the Gram-Schmidt signal in Fig. 9 of (a) **1·CH₃OH** and (b) **1·DMA** as well as reference spectra of (c) methanol and (d) N-dimethylacetamide.

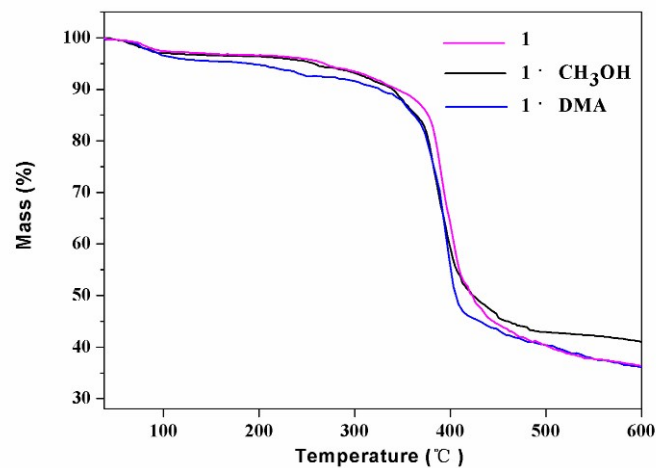


Fig. S11 TG curves for **1**, **1·CH₃OH** and **1·DMA** under a nitrogen atmosphere.

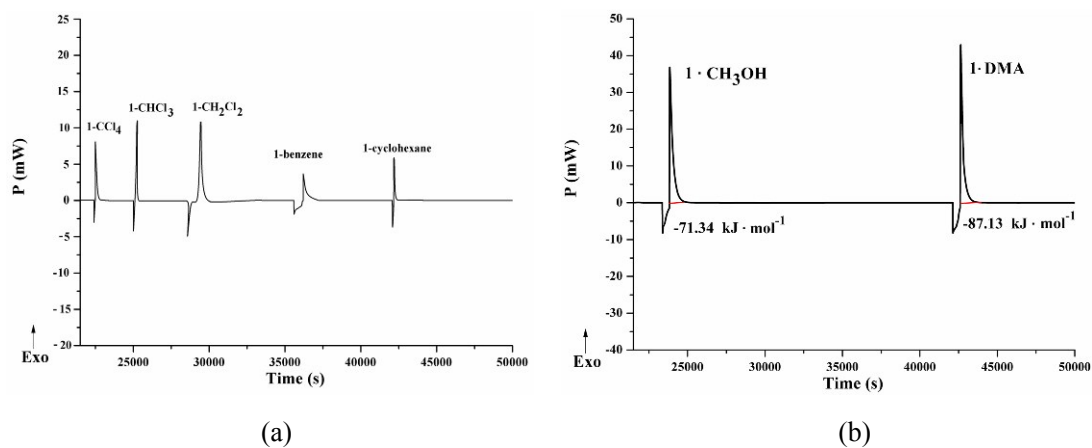


Fig. S12 (a) Variation of heat-flow as a function of time, **1·CH₂Cl₂**, **1·CHCl₃**, **1·CCl₄**, **1·benzene**, and **1·cyclohexane**, (b) **1·CH₃OH** and **1·DMA**.

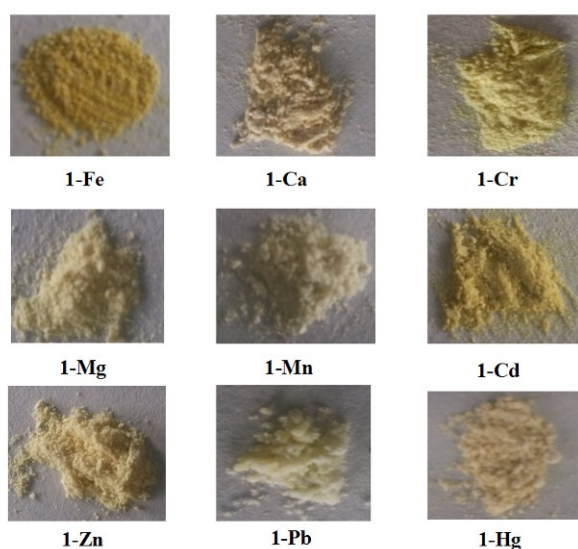
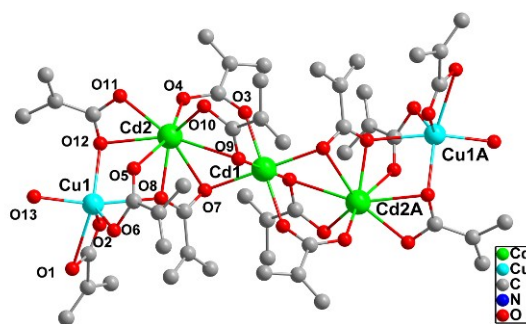
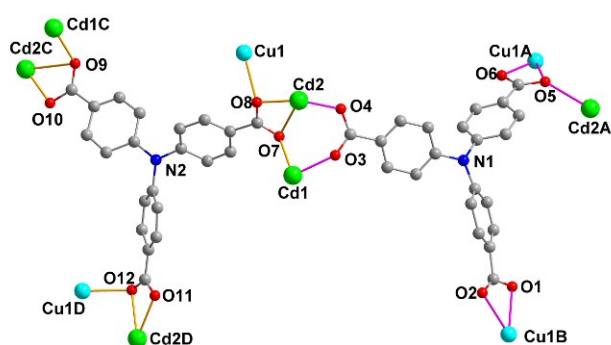


Fig. S13 Changes in color of addition of various metal ions (1×10^{-4} mol L⁻¹, 10 mL) to the crystals of **1**.

(a)



(b)



(c)

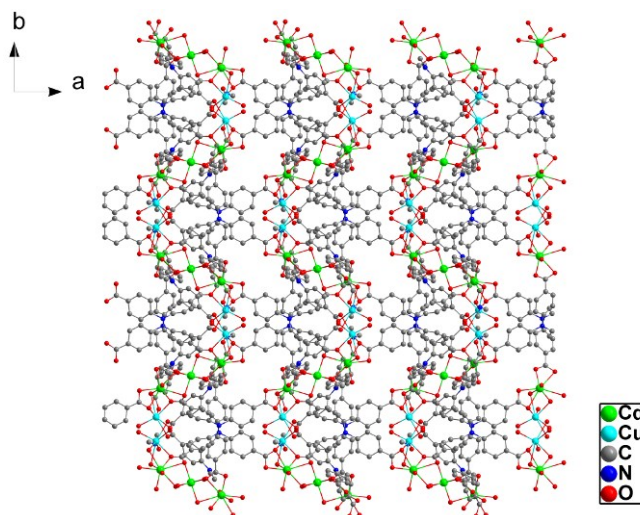


Fig. S14 (a) Coordination environments of the Cd(II) and Cu(II) ions in **2**. Symmetry code: A, $-x+1, -y, -z+2$; (b) Two different types of coordination modes of L^3 - ligand in **2**. Symmetry code: A, $x, y, z+1$; B, $-x+1, y-1/2, -z+5/2$; C, $-x+1, y+1/2, -z+3/2$; D, $x+1, y, z$; (c) View of the 3D framework of **2** shown in Ball-Stick mode along the c -axis. All H atoms, counter ions and solvent molecules are omitted for clarity.

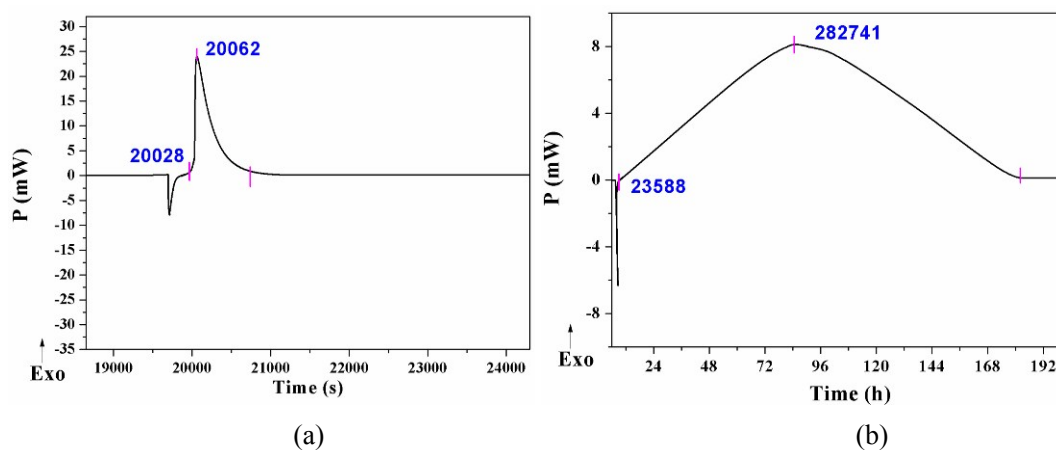


Fig. S15 (a) Variation of heat-flow as a function of time, $c(\text{Cu}^{2+}) = 1 \times 10^{-5} \text{ mol L}^{-1}$, (b) $c(\text{Cu}^{2+}) = 1 \times 10^{-6} \text{ mol L}^{-1}$.

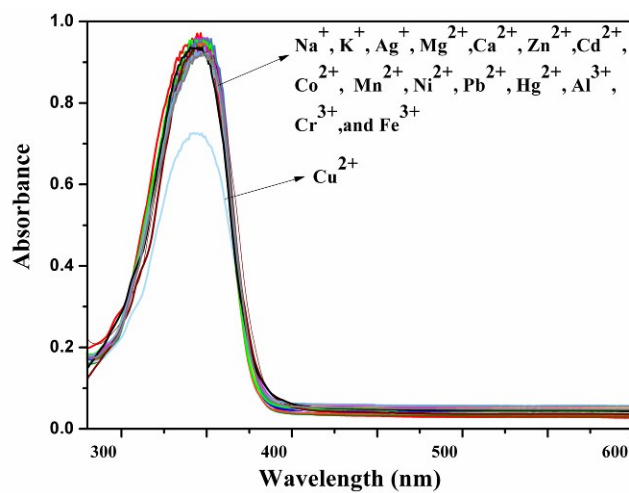


Fig. S16 Change in absorption intensity of 1 ($1 \times 10^{-5} \text{ M}$) in DMSO upon addition of various metal ions (10 mM).

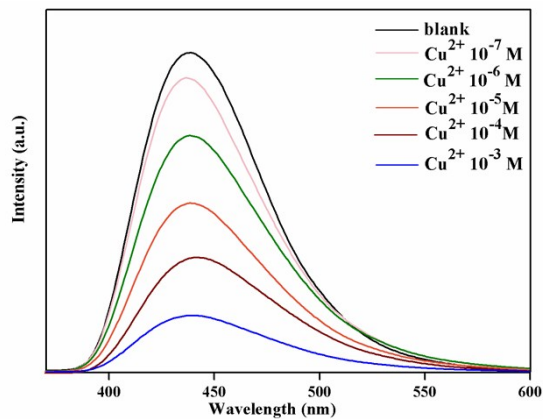


Fig. S17 Emission spectra of 1 in DMSO with $\text{Cu}(\text{NO}_3)_2$ at different concentrations.

Table S1 Crystal data and refinement parameters for compounds **1**, **2**, **1·CH₃OH** and **1·DMA**.

Compound	1	2	1·CH₃OH	1·DMA
Empirical formula	C ₈₈ H ₇₂ Cd ₅ N ₆ O ₂₈	C ₈₈ H ₇₂ Cd ₃ Cu ₂ N ₆ O ₂₇	C ₉₀ H ₇₆ Cd ₅ N ₆ O ₂₈	C ₉₆ H ₈₆ Cd ₅ N ₈ O ₂₈
Formula weight	2223.52	2109.80	2251.57	2361.73
Crystal system	Monoclinic	Monoclinic	Monoclinic	Monoclinic
Space group	<i>P2₁/c</i>	<i>P2₁/c</i>	<i>P2₁/c</i>	<i>P2₁/c</i>
<i>a</i> /Å	14.6261(6)	14.3997(19)	14.5830(13)	14.5196(9)
<i>b</i> /Å	23.2526(9)	23.362(3)	23.241(2)	23.3670(14)
<i>c</i> /Å	15.7357(7)	15.543(3)	15.6338(14)	15.6042(9)
<i>α</i> /°	90	90	90	90
<i>β</i> /°	107.099(2)	106.309(9)	106.990(2)	107.4750(10)
<i>γ</i> /°	90	90	90	90
<i>V</i> /Å ³	5115.1(4)	5018.2(12)	5067.4(8)	5049.8(5)
<i>Z</i>	2	2	2	2
<i>D_c</i> /(g·cm ⁻³)	1.444	1.396	1.476	1.553
<i>T</i> (K)	296(2)	296(2)	296(2)	296(2)
F(000)	2212	2120	2244	2364
Absorption coefficient/mm ⁻¹	1.094	1.114	1.106	1.114
Reflections collected/unique	27989 / 8921	28070 / 8802	19614 / 8639	24914 / 8877
<i>R</i> (int)	0.0320	0.1227	0.0463	0.0407
Goodness-of-fit on <i>F</i> ²	1.074	1.077	1.071	1.076
<i>R</i> ₁ ^a [<i>I</i> > 2σ(<i>I</i>)]	0.0487	0.1094	0.0563	0.0456
w <i>R</i> ₂ ^b (all data)	0.1717	0.3219	0.1818	0.1593
CCDC number	1417833	1417835	1424110	1417834

[^a] $R_1 = \sum ||F_o| - |F_c|| / \sum |F_o|$

[^b] $wR_2 = [\sum w(F_o^2 - F_c^2)^2 / \sum w(F_o^2)^2]^{1/2}$

References

- [S1] J. Wang, C. He, P. Y. Wu, J. Wang, C. Y. Duan, *J. Am. Chem. Soc.* **2011**, *133*, 12402–12405.
- [S2] M. Ji, M.Y. Liu, S.L. Gao, *Instrum. Sci. Technol.* **2001**, *29*, 53-57.
- [S3] V. K.J. Marthada, *Res. NBS Standards* **1980**, *85*, 467-470.
- [S4] S.L.Gao, Y. Fang, S.P. Chen, *Acta Chim. Sin.* **2002**, *60*, 2220-2224.
- [S5] Sheldrick, G. M. SADABS, Program for Empirical Absorption Correction; University of Göttingen, Göttingen, Germany, **1996**.
- [S6] Sheldrick, G. M. SHELXTL; Bruker Analytical X-ray Instruments Inc., Madison, WI, **1998**